Image Analysis by Discrete Orthogonal Hahn Moments*

Jian Zhou[1], Huazhong Shu[1], Hongqing Zhu[1],
Christine Toumoulin[2], and Limin Luo[1]

[1] Lab of Image Science and Technology,
Department of Biological Science and Medical Engineering, Southeast University,
210096 Nanjing, China
zjseu@hotmail.com, {shu.list, hqzhu, luo.list}@seu.edu.cn
[2] Laboratoire Traitement du Signal et de l'Image,
INSERM - Université de Rennes 1, Campus de Beaulieu,
35042 Rennes Cedex, France
christine.toumoulin@univ-rennes1.fr

Abstract. Orthogonal moments are recognized as useful tools for object representation and image analysis. It has been shown that the recently developed discrete orthogonal moments have better performance than the conventional continuous orthogonal moments. In this paper, a new set of discrete orthogonal polynomials, namely Hahn polynomials, are introduced. The related Hahn moment functions defined on this orthogonal basis set are investigated and applied to image reconstruction. In experiments, the Hahn moments are compared with the other two discrete orthogonal moments: Chebyshev and Krawtchouk moments. The simulation results show that the Hahn moment-based reconstruction method is superior to the other two discrete orthogonal moment-based methods.

1 Introduction

Moments and functions of moments have been widely used in pattern recognition [1],[2], image analysis [3], [4], [5], object representation [6], edge detection [7], [8] and texture analysis [9]. Examples of moment-based feature descriptors include the geometric moments, rotational moments, orthogonal moments and complex moments.

Orthogonal moments defined in terms of a set of orthogonal basis are often preferred due greatly to its ability to represent images with the minimum amount of information redundancy. Moment-based image reconstruction was pioneered by Teague who noted that image can be reconstructed from a set of orthogonal moments [3]. Since then, successive studies on orthogonal moments such as Legendre moment and Zenike moments for image reconstruction have

* This work was supported by the National Basic Research Program of China under grant No. 2003CB716102 and the National Natural Science Foundation of China under grant No. 60272045.

M. Kamel and A. Campilho (Eds.): ICIAR 2005, LNCS 3656, pp. 524–531, 2005.

been extensively addressed in [4] and [5]. However, these moments usually involve several major problems such as the numerical approximation of continuous integrals, coordinate space transformation, high computational costs and etc.

Recently, a set of discrete orthogonal moment functions based on discrete orthogonal polynomials, Chebyshev polynomials [10] and Krawtchouk polynomials [11] have been successfully introduced as alternatives to continuous orthogonal moments. The discrete orthogonal moments hold most of useful features embedded in the continuous orthogonal moments. Moreover, the implementation of discrete orthogonal moments does not require any numerical approximation since the basis set is orthogonal in the discrete domain of image coordinate space. Therefore, the accuracy of image reconstruction can be expectably better than the conventional continuous orthogonal moments.

In this paper, we will introduce a new set of discrete orthogonal moment functions which are characterized with the discrete orthogonal Hahn polynomials [12]. The resultant Hahn moment has most similar features to the Chebyshev and Krawtchouk moments, but it may outperform both the Chebyshev and Krawtchouk moments. The rest of paper is organized as follows: In Sect. 2, we introduce Hahn polynomials and the related Hahn moments, then briefly describe the computational aspects of the Hahn moments. In Sect. 3 we give out the experimental results. Finally, we conclude the paper.

2 Hahn Polynomials and Moments

2.1 Hahn Polynomials

For any integer $x \in [0, N-1]$(N is a given positive integer), Hahn polynomial of order n, $n = 0, 1, ..., N-1$, is defined as [12],

$$h_n^{(\mu,\nu)}(x, N) = (N+\nu-1)_n (N-1)_n \times \sum_{k=0}^{n} (-1)^k \frac{(-n)_k (-x)_k (2N+\mu+\nu-n-1)_k}{(N+\nu-1)_k (N-1)_k} \frac{1}{k!}, \quad (1)$$

where $(a)_k = a \cdot (a+1) \cdots (a+k-1) = \frac{\Gamma(a+k)}{\Gamma(a)}$ is the Pochhammer symbol and μ, ν ($\mu > -1, \nu > -1$) are adjustable parameters controlling the shape of polynomials. The discrete Hahn polynomials satisfy the following orthogonal condition:

$$\sum_{x=0}^{N-1} \rho(x) h_m^{(\mu,\nu)}(x, N) h_n^{(\mu,\nu)}(x, N) = d_n^2 \delta_{mn}, \quad 0 \le m, n \le N-1, \quad (2)$$

where δ_{mn} denotes the Dirac function, $\rho(x)$ is so-called weighting function which is given by

$$\rho(x) = \frac{1}{\Gamma(x+1)\Gamma(x+\mu+1)\Gamma(N+\nu-x)\Gamma(N-n-x)} \quad (3)$$

and the square norm d_n^2 has the following expression

$$d_n^2 = \frac{\Gamma(2N+\mu+\nu-n)}{(2N+\mu+\nu-2n-1)\Gamma(N+\mu+\nu-n)} \times \frac{1}{\Gamma(N+\mu-n)\Gamma(N+\nu-n)\Gamma(n+1)\Gamma(N-n)}. \quad (4)$$

To avoid numerical fluctuations in moment computation, we usually scale the Hahn polynomials by utilizing the square norm and the weighting function, i.e.,

$$\tilde{h}_n^{(\mu,\nu)}(x,N) = h_n^{(\mu,\nu)}(x,N)\sqrt{\frac{\rho(x)}{d_n^2}}, \quad n = 0,1,...,N-1. \quad (5)$$

Therefore, the orthogonal property of normalized Hahn polynomials can be described as

$$\sum_{x=0}^{N-1} \tilde{h}_m^{(\mu,\nu)}(x,N)\tilde{h}_n^{(\mu,\nu)}(x,N) = \delta_{mn}, \quad 0 \le m,n \le N-1. \quad (6)$$

2.2 Hahn Moments of Image

Given a digitalized image $f(x,y)$ with size $N \times N$, the $(m+n)$th order of Hahn moment of image is

$$H_{mn} = \sum_{x=0}^{N-1}\sum_{y=0}^{N-1} f(x,y)\tilde{h}_m^{(\mu,\nu)}(x,N)\tilde{h}_n^{(\mu,\nu)}(y,N), \quad m,n = 0,1,...,N-1. \quad (7)$$

Using (6), Eq.(7) leads to the following inverse moment transform

$$f(x,y) = \sum_{m=0}^{N-1}\sum_{n=0}^{N-1} H_{mn}\tilde{h}_m^{(\mu,\nu)}(x,N)\tilde{h}_n^{(\mu,\nu)}(y,N). \quad (8)$$

It indicates that the image can be completely reconstructed by calculating its discrete orthogonal moments up to order $2N-2$. This property makes the discrete orthogonal moments superior to the conventional continuous orthogonal moments. If moments are limited to an order M, we can approximate f by $\hat{f}$

$$\hat{f}(x,y) = \sum_{m=0}^{M}\sum_{n=0}^{M} H_{m-n,n}\tilde{h}_{m-n}^{(\mu,\nu)}(x,N)\tilde{h}_n^{(\mu,\nu)}(y,N), \quad x,y = 0,1,...,N-1. \quad (9)$$

2.3 Computational Aspects

Using (1) and (5), the zero-order and first-order normalized Hahn polynomials can be easily calculated, i.e.,

$$\tilde{h}_0^{(\mu,\nu)}(x,N) = \sqrt{\frac{\rho(x)}{d_0^2}}, \quad (10)$$

$$\tilde{h}_1^{(\mu,\nu)}(x,N) = \left\{(N+\nu-1)(N-1) - (2N+\mu+\nu-2)x\right\}\sqrt{\frac{\rho(x)}{d_1^2}}. \quad (11)$$

Higher orders polynomials can be deduced from the following recursive relations,

$$A\tilde{h}_n^{(\mu,\nu)}(x,N) = B\sqrt{\frac{d_{n-1}^2}{d_n^2}}\ \tilde{h}_{n-1}^{(\mu,\nu)}(x,N) + C\sqrt{\frac{d_{n-2}^2}{d_n^2}}\ \tilde{h}_{n-2}^{(\mu,\nu)}(x,N),$$
$$n = 2,3,...,N-1, \quad (12)$$

where

$$A = -\frac{n(2N+\mu+\nu-n)}{(2N+\mu+\nu-2n+1)(2N+\mu+\nu-2n)}, \quad (13)$$

$$B = x - \frac{2(N-1)+\nu-\mu}{4} - \frac{(\mu^2-\nu^2)(2N+\mu+\nu)}{4(2N+\mu+\nu-2n+2)(2N+\mu+\nu-2n)}, \quad (14)$$

$$C = \frac{(N-n+1)(N-n+\mu+1)(N-n+\nu+1)(N-n+\mu+\nu+1)}{(2N+\mu+\nu-2n+2)(2N+\mu+\nu-2n+1)}. \quad (15)$$

Equations (10)-(15) can be used to efficiently calculate the normalized Hahn moment of any order. Also the weighting function $\rho(x)$ can be solved by using the recursive relation with respect to x, i.e.,

$$\rho(x) = \frac{(N-x)(N+\nu-x)}{x(x+\mu)}\rho(x-1), \quad x = 1,2,...,N-1, \quad (16)$$

with

$$\rho(0) = \frac{1}{\Gamma(\mu+1)\Gamma(N+\nu)\Gamma(N-n)}. \quad (17)$$

To extract the image moment set $\{H_{mn}\}(0 \le m,n \le N-1)$, we can simply use the following matrix notation,

$$\mathbf{H} = \mathbf{H}_x^T\ \mathbf{f}\ \mathbf{H}_y \quad (18)$$

where $\mathbf{f}$ denotes the $N \times N$ image matrix and

$$\mathbf{H}_x = \left[\tilde{h}_0^{(\mu,\nu)}(x,N), \tilde{h}_1^{(\mu,\nu)}(x,N), \cdots, \tilde{h}_{N-1}^{(\mu,\nu)}(x,N)\right]^T,$$

$$\mathbf{H}_y = \left[\tilde{h}_0^{(\mu,\nu)}(y,N), \tilde{h}_1^{(\mu,\nu)}(y,N), \cdots, \tilde{h}_{N-1}^{(\mu,\nu)}(y,N)\right]^T$$

and

$$\tilde{h}_n^{(\mu,\nu)}(x,N) = \left[\tilde{h}_n^{(\mu,\nu)}(0,N), \tilde{h}_n^{(\mu,\nu)}(1,N), \cdots, \tilde{h}_n^{(\mu,\nu)}(N-1,N)\right]^T,$$
$$n = 0,1,...,N-1. \quad (19)$$

Similarly, the inverse reconstruction procedure can be represented as

$$\mathbf{f} = \mathbf{H}_x\ \mathbf{H}\ \mathbf{H}_y^T \quad (20)$$

Fig. 1. Test images. The left is binary image of Chinese character (size: 48×48) and the right is the standard gray image of Lena (size: 96×96).

To approximate the image with limited moments of order up to M, we need only to compute

$$\widetilde{\mathbf{H}}_x = \left[\tilde{h}_0^{(\mu,\nu)}(x,N), \tilde{h}_1^{(\mu,\nu)}(x,N), \cdots, \tilde{h}_M^{(\mu,\nu)}(x,N)\right]^T,$$

$$\widetilde{\mathbf{H}}_y = \left[\tilde{h}_0^{(\mu,\nu)}(y,N), \tilde{h}_1^{(\mu,\nu)}(y,N), \cdots, \tilde{h}_M^{(\mu,\nu)}(y,N)\right]^T$$

and then yield the moment matrix $\mathbf{H}$ using (18). The approximation of image, say $\hat{\mathbf{f}}$, can be solved by the analogous way as shown in (20).

Noticed that the normalized Hahn polynomials are unavoidably related to weighting function $\rho(x)$. For the case of image reconstruction, we usually expect that the Hahn polynomials are symmetric (odd or even) with respect to the center point $(x, y) = (N/2, N/2)$ (suppose N is even). As a result, we require the same values for both μ and ν. For the sake of simplicity, we choose $\mu = \nu = 0$.

3 Experimental Results

To evaluate the performance of image reconstruction using Hahn moments, we have selected several test images including the binary image and the gray level image (shown in Fig. 1). Reconstruction results are compared with those using Chebyshev and Krawtchouk moments. Noisy images are also considered to analyze the noise sensitivity of these different moment-based reconstruction methods.

The mean square error (MSE) is used as the fidelity criteria measuring the resemblance between the reconstructed images and the original one. It can be defined by

$$\text{MSE} = \frac{||\boldsymbol{f} - \boldsymbol{f}^*||^2}{||\boldsymbol{f}^*||^2} \tag{21}$$

where $||\cdot||$ is the standard Euclidean norm and $\boldsymbol{f}^*$ represents the original image vector and $\boldsymbol{f}$ the reconstructed image vector.

Fig. 2 shows reconstructions using three different discrete orthogonal moments and the corresponding MSE comparison through the reconstruction procedure is depicted in Fig. 3. We observe that the reconstruction based on Hahn

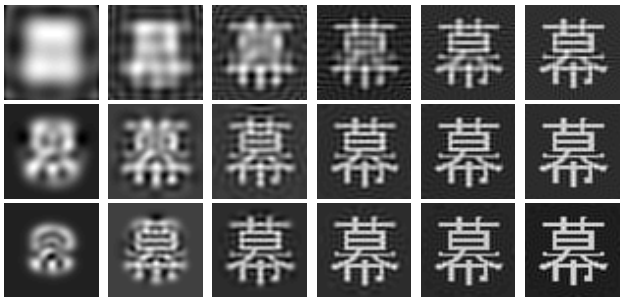

Fig. 2. Reconstructions using Chebyshev moments (first row), Krawtchouk moments (second row, $p = 0.5$ [11]) and Hahn moments (third row, $\mu = \nu = 0$). The orders from the left column to the right are 8, 16, 24, 32 and 47 respectively.

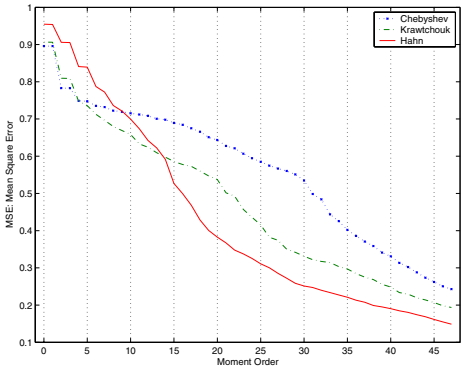

Fig. 3. Comparisons of the binary image reconstruction results

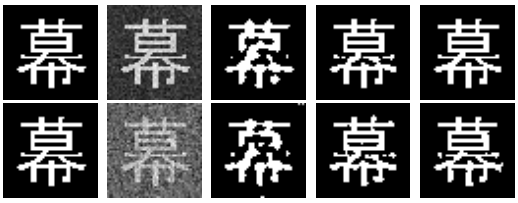

Fig. 4. Reconstructions using Gaussian noise-contaminated binary image where the maximum order is all fixed at 30. From left column to right column are: original images, noisy images, and reconstructions using Chebyshev, Krawtchouk ($p = 0.5$ [11]), Hahn moments ($\mu = \nu = 0$) respectively. The noise variance in the first row is 0.1 and the second row 0.3.

moment function may outperform the other two types of discrete orthogonal moments.

In Fig. 4, we test the noise robustness of different orthogonal moments. Gaussian noises with different variances have been added to the original binary image

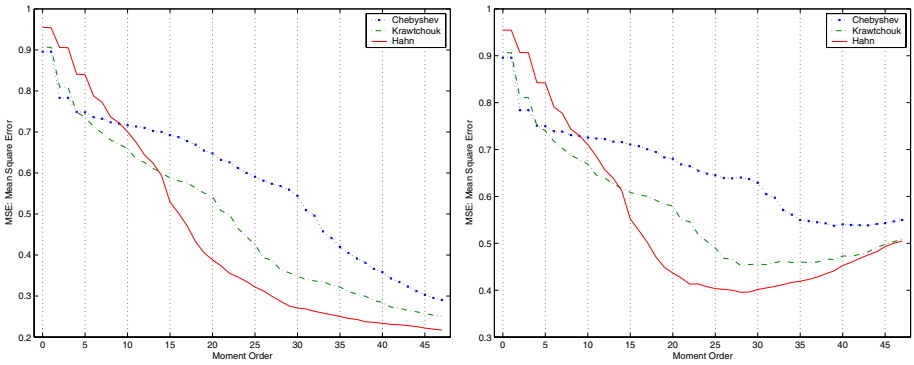

Fig. 5. Noisy binary image reconstruction MSE comparison where Gaussian noise with zero mean, variance: the left 0.1 and the right 0.3

(a) MSE: 0.1164 (b) MSE: 0.0830 (c) MSE: 0.0762

Fig. 6. Reconstructions of image Lena using (a) Chebyshev moments, (b) Krawtchouk moments ($p = 0.5$ [11]) and (c) Hahn moments ($\mu = \nu = 0$) respectively. Moments up to order 75 are used.

of Chinese character. All of the reconstructions have been normalized to binary values with the same threshold 0.5. The MSE's shown in Fig. 5 again indicate the better performance of Hahn moments even if the image is contaminated with slightly large variance Gaussian noise. In Fig. 5, we can see that the increasing order moment may inversely degrade the image when image signal-to-noise rate (SNR) is relatively low.

Fig. 6 shows the approximation of gray level image. Clearly, the Hahn moment based method can yield slightly lower MSE than the other two orthogonal moments. It may indicate the best performance of discrete orthogonal Hahn moments in image reconstruction.

4 Conclusions

In this paper, we have introduced a new set of discrete orthogonal polynomials, namely Hahn polynomials. The corresponding Hahn moment functions defined on this basis set were then investigated and applied to image reconstruction. In

experimental studies, we have compared our Hahn moment based reconstruction method with the other two discrete orthogonal moments, Chebyshev and Krawtchok moments based method. The results have shown the best performance of Hahn moment based method.

References

1. Lo, C. H., Don, H. S.: 3D moment forms: Their construction and application to object identification and positioning, IEEE Trans. Pattern Anal. Mach. Intell. **11** (1989), 1053–1064.
2. Flusser, J., Suk, T.: Pattern Recognition by affine moment invariants, Pattern Recognition, **26** (1993), 167–174.
3. Teague, M. R.: Image analysis via the general theory of moments, J. Opt. Soc. Am. **70** (1980), 920–930.
4. Teh, C. H., Chin, R. T.: On Image analysis by the method of moments, IEEE Trans. Pattern Anal. Mach. Intell. **10** (1988), 485–513.
5. Liao, S. X., Pawlak, M.: On image analysis by moments, IEEE Trans. Pattern Anal. Mach. Intell. **18** (1996), 254–266.
6. Papademetriou, R. C.: Reconstructing with moments, Proceedings of 11th International Conference, Pattern Recognition (1992) 476–480.
7. Luo, L. M., Hamitouche, C., Dilenseger, J. L., Coatrieux, J. L.: A moment-based three-dimensional edge operator, IEEE Trans. Biomed. Eng. **40** (1993), 693–703.
8. Luo, L. M., Xie, X. H., Bao, X. D.: A modified moment-based edge operator for rectangular pixel image, IEEE Trans. Circuits Systems Video Technol. **4** (1994), 552–554.
9. Tuceryan, M.: Moment-based texture segmentation, Pattern Recognition Lett. **15** (1994), 115–123.
10. Mukundan, R., Ong, S. H., Lee, P. A.: Image analysis by Tchebichef moments, IEEE Trans. Imag. Proc. **10(9)** (2001), 1357–1364.
11. Yap, P. T., Paramesran, R., Ong, S. H.: Image analysis by Krawtchouk moments, IEEE Trans. Imag. Proc. **12(11)** (2003), 1367–1377.
12. Nikiforov, A. F., Uvarov, V. B., Special functions of mathematical physics, Birkhäuser, Basel Boston, (1988).